MTLA 39 (2025) 102317

Contents lists available at ScienceDirect

Materialia

journal homepage: www.elsevier.com/locate/mtla

An extraordinarily low-energy threshold of less than 60 keV for ion track formation in silicon

H. Amekura [a,*], K. Narumi [b], A. Chiba [b], Y. Hirano [b], K. Yamada [b], S. Yamamoto [b], Y. Saitoh [b]

[a] National Institute for Materials Science (NIMS), Tsukuba, 305-0003, Japan
[b] Takasaki Institute for Advanced Quantum Science, National Institutes for Quantum Science and Technology (QST), Takasaki, 370-1292, Japan

ARTICLE INFO

Keywords:
Ion track
C_{60} ion
Silicon
Cluster effect
Swift heavy ion

ABSTRACT

The impingement of a C_{60} cluster ion upon a solid can realize the temporospatially correlated injection of sixty C atoms to the solid at the same time and place with a molecular dimension of 0.7 nm in diameter. This could result in ion track formation that differs from that of conventional monatomic ion irradiation. Although no ion tracks have been observed in Si even under high-energy 3.6-GeV monatomic U ion irradiation, certain tracks have been found in Si under low-energy 1-MeV C_{60} ion irradiation. Here, we investigated track formation under an irradiation of less than 1 MeV: (i) With a decrease in energy, the diameters and lengths of the tracks decreased; however, the length decreased more steeply than the diameter. (ii) Although the tracks were fuzzily perceived down to 60-keV irradiation, no tracks were observed under 30-keV irradiation, except for an extended damage zone. Furthermore, we observed (iii) track formation below the electronic stopping threshold, and (iv) track length extension due to "the acceleration effect" of cluster-ion irradiation at low energies. (v) Finally, the approximated linearity between the track volume and C_{60} energy is discussed.

1. Introduction

Crystalline Si is one of the most investigated materials, particularly regarding its ion–solid interactions in the energy range from sub-keV to several MeV. This is because ion implantation into Si is one of the most important processes in fabricating micro-/nano-integrated circuits for information technologies [1]. Nevertheless, ion track formation in crystalline Si under high-energy heavy ions of nearly 1 MeV/amu or higher, which are called swift heavy ions (SHIs), has remained controversial [2–14].

Although various SHI irradiations have been attempted to find track formation in Si [2,3], tracks have never been observed even when irradiated with high-energy 3.6-GeV U ions (electronic energy loss S_e = 23.7 keV/nm) [3]. This is close to the Bragg peak, i.e., the highest S_e attainable in Si by monatomic SHIs (m-SHIs). It should be noted that the reported S_e values are shown herein after recalculation using the SRIM 2013 code [15]. This indicates that ion tracks are not formed in Si by m-SHIs; however, tracks have been observed in Si under 30- and 40-MeV C_{60} fullerene cluster ion irradiation in the Orsay facility, France [4,5]. The 30- and 40-MeV C_{60} ions afford a high S_e of 42.7 and 50.0 keV/nm in Si, respectively. Thus, many researchers believed that not observing track formation in Si under m-SHI irradiation is ascribable to the considerably high S_e threshold in Si, which cannot be overcome by m-SHIs, except by extremely high S_e delivered by C_{60} ions. Considering that 60 carbon atoms from a C_{60} molecule were simultaneously injected into a solid, a significantly higher S_e was obtained even with C_{60} ions having tens MeV [16–18].

Furthermore, the pioneer papers of the first observation of tracks in Si using C_{60} ions by Canut et al. [4] and Dunlop et al. [5] have already pointed out the importance of the velocity effect. Much slower velocity of C_{60} ions compared to that of m-SHIs may induce much higher excitation density for the track formation in former ions. The inelastic thermal spike (i-TS) calculations [19] by Chettah et al. [6], which include the velocity effect, however, suggest that the calculated velocity effect is not high enough to explain the completely different track formations between C_{60} ions and m-SHIs if the tracks are formed by melting.

The i-TS calculations raised further the mystery of the ion tracks in Si [6]. Following the melting criterion for the track formation, the S_e threshold was estimated as low as ~5 keV/nm. This quite low threshold is inconsistent with all of the past experiments where the tracks were formed only higher than 25 keV/nm. The experimental results under

* Corresponding author at: National Institute for Materials Science (NIMS), 3-13 Sakura, Tsukuba, 305-0003, Japan.
E-mail address: amekura.hiroshi@nims.go.jp (H. Amekura).

https://doi.org/10.1016/j.mtla.2024.102317
Received 26 August 2024; Accepted 9 December 2024
Available online 9 December 2024

20–40 MeV C_{60} irradiations were rather reproduced by the vaporization criterion. Then, raised questions are (i) "why the melting zones do *not* transform to the ion tracks but disappear" and (ii) "whether the prerequisites of the present i-TS model are applicable to semiconductor Si or not." Similar results were reported from another group using the i-TS model with Monte Carlo electron dynamics [7], instead of Waligorski distribution [20], indicating that the discrepancy between the calculations and experiments is not accidental but could be due to an intrinsic imperfection of the i-TS model presumed.

To answer the question (i), the recrystallization of tracks in Si was proposed [8]. Since the recrystallization of Si is often observed under low energy ion irradiation, i.e., the nuclear stopping regime, the same phenomenon can be induced on the electronic stopping regime [8]. While the tracks are transiently formed in Si via the melting, soon the tracks disappear by the recrystallization of Si before experimental observation begins.

Regarding (ii), one of the imperfections of the i-TS model was pointed out: In the i-TS model, the carrier relaxation via the bandgap is not considered [21]. This assumption sounds too crude to obtain reliable results, while many successes were reported from the track formations in bandgap materials, i.e., many insulators and some semiconductors [19]. Duffy and coworkers extended the i-TS model including the carrier relaxation via bandgap [21]. Since the calculations became much more difficult than the standard i-TS model, some rough approximations were introduced. Assuming the electron-phonon relaxation time of 0.4 ps, the experimental results of 30–40 MeV C_{60} irradiations have been reproduced by the *melting criterion* with the S_e threshold of 25 keV/nm [21]. This was inconsistent with our results in the previous paper where the tracks were formed under 1–9 MeV C_{60} irradiations, i.e., $S_e = 7.5$–21.3 keV/nm [9]. Improvements of the ion track calculations applicable to Si were also discussed by other authors [22,23], including the non-thermal melting model [23].

One of the recent remarkable observations was reported by Dürr et al. [10], who irradiated hydrogen-terminated Si surface with m-SHIs. While they observed the H-terminated Si surface by Scanning Tunneling Microscope (STM) after SHI irradiation, they occasionally observed loss of one or two atoms only. If a melting track would be formed in Si, the terminated hydrogen atoms on the surface of several nm in diameter could be lost, since the Si-H bonds are easily ruptured at such high temperatures [10]. Since the hydrogen loss from the surface is an irreversible process, the lost hydrogen atoms have never returned even if the perfect recrystallization of Si would be induced after cooling. Therefore, their results are inconsistent with the melting (and vaporization) in Si.

In our recent publications, we reported track formation in Si under C_{60} irradiations in the range of 1–9 MeV [9,11], which has considerably lower energies than the C_{60} irradiation of 20–40 MeV performed in the Orsay facility [4,5]. Nevertheless, tracks were formed in Si under 1-MeV C_{60} ion irradiation ($S_e = 7.5$ keV/nm), while 3.6-GeV monatomic U ion irradiation (23.7 keV/nm) does not.

This paper reports the investigation of track formation in Si irradiated with C_{60} ions in the energy region below 1 MeV (i.e., 30–750 keV), as we successfully observed ion tracks under 1-MeV C_{60} irradiation in previous studies [9,11]. Since the acceleration of C_{60} ions to less than 1 MeV was difficult for a 3-MV tandem accelerator, a 400-kV single-ended ion implanter was used here. Although Si is known to be tolerant to track formation by m-SHI irradiation, tracks were observed down to 60-keV C_{60} ions ($S_e = 1.8$ keV/nm). The extrapolated S_e threshold from the C_{60} irradiation data of 1–9 MeV was ~4 keV/nm; therefore, track formation under 60-keV C_{60} irradiation ($S_e = 1.8$ keV/nm) cannot be explained by S_e only. A contribution from the nuclear energy deposition (S_n) or something else cannot be excluded. At low energies, the track lengths increase beyond those expected from the ion range of individual ions, which can be a manifestation of "the acceleration effect" of cluster ions [24,25]. The approximated linearity between the track volume and ion energy is discussed.

2. Experimental

Samples of single crystalline Si were cut from commercially available wafers of p-type conduction (boron-doped) with a resistivity of ~1 Ω cm, grown via the Czochralski method. The samples were mechanically cut into 3 mm × 4 mm rectangles, which were called bulk samples. The bulk samples were immersed in hydrofluoric acid to remove surface oxide.

The tracks were evaluated by transmission electron microscopy (TEM), and two configurations of TEM samples were prepared [9,11,26]. Top-view samples were obtained by thinning down an unirradiated bulk sample to a thickness of less than ~100 nm using 30-keV Ga focused ion beam (FIB) milling and held on TEM grids. The top-view samples on the grids were irradiated with C_{60} ions at an incident angle of 7° from the surface normal, to observe the track diameters by TEM.

Side-view samples were obtained by irradiating the 3 mm × 4 mm faces of other bulk samples with C_{60} ions at an incident angle of 7° from the surface normal. Thereafter, the side-view samples were picked up from the irradiated surfaces and thinned down along the C_{60} beam by FIB to observe the depth profiles of the ion tracks. To identify the surface location of the side-view samples, a thin Pt layer was deposited on the sample surfaces prior to the FIB thinning. An amorphous C layer was subsequently deposited over the Pt layer to protect it from FIB milling.

The irradiation of C_{60} ions was conducted at the Takasaki Institute for Advanced Quantum Science, of the National Institutes for Quantum Science and Technology (QST). A 400-kV single-ended ion implanter and a 3-MV tandem accelerator were used for energy ranges of 30–750 keV and 1–9 MeV, respectively. This study focused on the former energy range. The details of irradiation in the latter energy range are available elsewhere [9,11].

C_{60} ions of 30–120, 200–540, and 750 keV were accelerated under the maximum voltage of 400 kV using the different charge states of C_{60}^{+}, C_{60}^{2+}, and C_{60}^{3+}, respectively. The C_{60} ions of 1–6 MeV and 9 MeV were accelerated by the 3 MV tandem accelerator using the charge states of C_{60}^{+} and C_{60}^{2+}, respectively. The energies and the initial charge states were summarized in Table 1. The fluence was set to 5×10^{10} or 1×10^{11} C_{60}/cm^2 to avoid the overlap of the tracks. To improve the beam homogeneity, the C_{60} beams were horizontally and vertically scanned at frequencies of 89 and 502 Hz, respectively. An ion flux was adjusted between 0.3 and 1 nA, with an irradiation area of ~0.5 cm^2.

TEM observation was conducted using a JEOL JEM-2100 microscope, with an operating voltage of 200 kV. Approximately fifty tracks each were examined to determine either the mean diameter and the mean length for every ion energy. According to past literature [5], the tracks in Si were recrystallized with prolonged TEM observation. Careful observations were performed to minimized the electron current and observation time. It was confirmed that any apparent changes were not

Table 1
Comparison of the experimental initial charges Q_{in} of C_{60} ions and the effective charges Q_{eff} calculated by Shima's formula [30]. The numbers with underline indicate the regions where $Q_{eff} \sim Q_{in}$.

C_{60} energy (MeV)	Q_{in}	Q_{eff}	Q_{eff} / Q_{in}
9	+2	13.3	6.66
6	+1	10.9	10.9
4	+1	8.97	8.97
3	+1	7.78	7.78
2	+1	6.37	6.37
1	+1	4.53	4.53
0.75	+3	3.92	1.31
0.5	+2	3.21	1.61
0.4	+2	2.87	1.44
0.2	+1	2.04	2.04
0.12	+1	1.58	1.58
0.06	+1	1.12	1.12
0.03	+1	0.790	0.790

induced during the observation.

The stopping powers of m-SHI were calculated using the SRIM 2013 code [15]; those of the C_{60} ion were determined using the following relationship:

$$S_i(E, C_{60}) = \gamma_i N S_i(E/N, C_1) \quad (1)$$

where $i = e$ (electronic) [16], and $i = n$ (nuclear) [27]; $N = 60$ was presumed for C_{60} ions. Eq. (1) shows that the stopping power of a C_{60} ion is equal to $\gamma_i N$ times that of a monatomic C ion with the same velocity as the C_{60} ion. Although $\gamma_i = 1$ is frequently assumed, the assumption of $\gamma_e \sim 1$ was recently bolstered by Kaneko's calculations [17], which concluded that γ_e was approximated as a constant of 0.8 between 2- and 10-MeV C_{60} ions in carbon foil. Here, $\gamma_e = 1$ was assumed in Eq. (1) to maintain consistency with our previous papers [9,11,18,26].

Since the SRIM code was used to determine the stopping powers, the attainment to the effective charges was assumed. However, this is not trivial for m-SHIs [28]. How about C_{60} ions? Furthermore, since very short tracks, which are formed by low-energy C_{60} ions, are one of the main concerns of the present work, the charge equilibrium thickness should be estimated. Toulemonde [29] studied the equilibrium thickness of m-SHIs, and proposed a relationship between the specific energy E_p (MeV/u) and the thickness of carbon stripper foil X_{66} required for the charge equilibrium as,

$$X_{66}\left[\mu g/cm^2\right] = 5.0\left(E_p[MeV/u]\right)^{1.5}. \quad (2)$$

In the original paper [29], he used the pre-factor of 2.5 instead of 5.0. However, since he suggested in the same paper to double the value for certainty, we used the pre-factor of 5.0. Of course, since this relationship is determined form the data between 1 and 44 MeV/amu, it is not guaranteed to apply slow C_{60} ions of much lower than 1 MeV/amu. However, the application of this relationship could provide a rough estimation. When $E_p = 1$ MeV/amu, the foil of 5 μg/cm^2, i.e., 23 nm in thickness, is required, which sounds reasonable. The amorphous carbon density of 2.2 g/cm^3 was used. In the case of our highest energy of 9 MeV C_{60} ion (0.0125 MeV/u), the foil of 0.006 μg/cm^2, i.e., 0.03 nm in thickness, was calculated. While this thickness was calculated in a carbon foil, which could be different in Si, the charge equilibrium could be attained also in Si within a considerably thin surface layer, which is much shorter than the observed track lengths. The most parts of the tracks are formed under the charge equilibrium.

The effective charges Q_{eff} of C_{60} ions were estimated from the ion velocities v with applying the formula proposed by Shima et al. [30], i.e.,

$$Q_{eff} = Z_1\left[1 - \exp\left(-1.25v_r + 0.32v_r^2 - 0.11v_r^3\right)\right]g(Z_2) \quad (3)$$

with

$$v_r = 0.608(v/v_B)/Z_1^{0.45} \quad (4)$$

$$g(Z_2) = 1 - 0.0019(Z_2 - 6)v_r^{0.5} + 10^{-5}(Z_2 - 6)^2 v_r \quad (5)$$

where Z_1, Z_2, and v_B denote the charge numbers of the projectile and of the target, and the Bohr velocity, respectively. The effective charges Q_{eff}

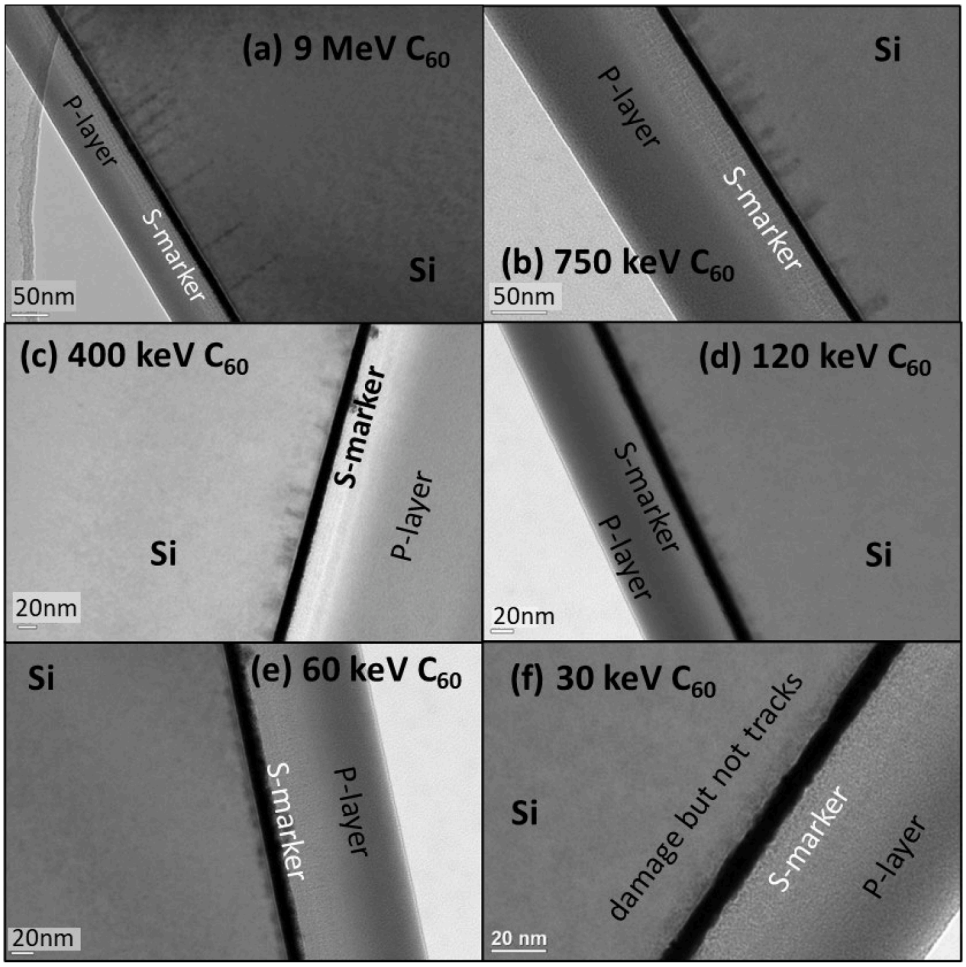

Fig. 1. Side-view bright-field transmission electron microscopy (BF-TEM) images of ion tracks in Si, which were irradiated with C_{60} ions of energies ranging from 9 MeV to 30 keV. The samples were irradiated to a fluence of 1×10^{11} C_{60}/cm^2 except to 5×10^{10} C_{60}/cm^2 at 750 keV and 9 MeV. The black thin layers are Pt films deposited as surface markers. The P-layers are protection layers against FIB, made of deposited amorphous C.

of C_{60} ions in various energies were calculated and compared with the experimental initial charges Q_{in} as shown in Table 1.

Since the ratio Q_{eff} / Q_{in} for 750 keV C_{60} ions or less is approximated to ~1.4, the ions were injected with the charges relatively close to the effective ones. Charge redistributions to the equilibriums could be modest. Contrary, since the ratio Q_{eff} / Q_{in} is much higher than the unity for 1 MeV C_{60} ions or higher energies, relatively large charge redistributions were induced within a shallow surface layer.

3. Results

Fig. 1 shows side-view bright-field TEM (BF-TEM) images of ion tracks in Si. The samples were irradiated with C_{60} ions of energies ranging from 30 keV to 9 MeV. A fluence of 1×10^{11} C_{60}/cm^2 was applied, except 5×10^{10} C_{60}/cm^2 for 750 keV and 9 MeV. The thin black layer located approximately at the center of each figure was a Pt film deposited as a surface marker. Protection layers (P-layers), made of amorphous C, against FIB thinning were deposited over the Pt layers.

Ion tracks were observed as black cylinders close to the other side of the Pt layers. The longest cylinders with the highest aspect ratio (*AR*) were observed at the highest energy of 9 MeV. With a decrease in the ion energy, the *AR* of the tracks decreased, i.e., the track length *steeply* decreased, but the diameter *gradually* decreased.

With a decrease in energy, the *AR* of the tracks decreased, i.e., the shapes became slightly rounder, probably indicating a crossover from the electronic *cylindrical* tracks to nuclear *spherical* tracks. With a decrease in energy to 120 keV or lower, the tracks did not appear cylindrical but rather elongated semi-spherical. However, isolated tracks with low *AR*s were perceived down to 60 keV. A nearly continuous damaged layer, instead of isolated tracks, was observed beneath the Pt layer under 30-keV irradiation. Thus, isolated tracks were no longer observed under 30-keV irradiation.

Fig. 2 shows the top-view images of the ion tracks in Si, with white dots representing the tracks. The colors of the dots were confirmed to change from white to black with the defocusing of TEM, indicating that the dots were due to the Fresnel contrast and have lower density than the matrix, attributable to the ion tracks. The white dots were easily observed down to 120 keV. As the dots became smaller, the images became less clear but were still observed under an irradiation of 60 keV. However, they were not observed under 30-keV irradiation.

Figs. 1 and 2 show that ion tracks were formed down to 60-keV irradiation but not under 30-keV irradiation. Instead, a continuous damaged layer was observed under 30-keV irradiation, as shown in Fig. 1(f).

After analyzing the TEM images of the ion tracks, the mean track length (*L*), mean track diameter (*D*), and their standard deviations (SDs) were determined and are plotted in Fig. 3 against the ion energy. *L* and *D* were determined from the side- and top-view TEM images, respectively. The ion energy (*E*) dependences were fitted by power-law dependences with adjustments in the exponents:

$$L \propto E^{P} \text{ with } P = 0.397 \quad (6)$$

$$D \propto E^{Q} \text{ with } Q = 0.209. \quad (7)$$

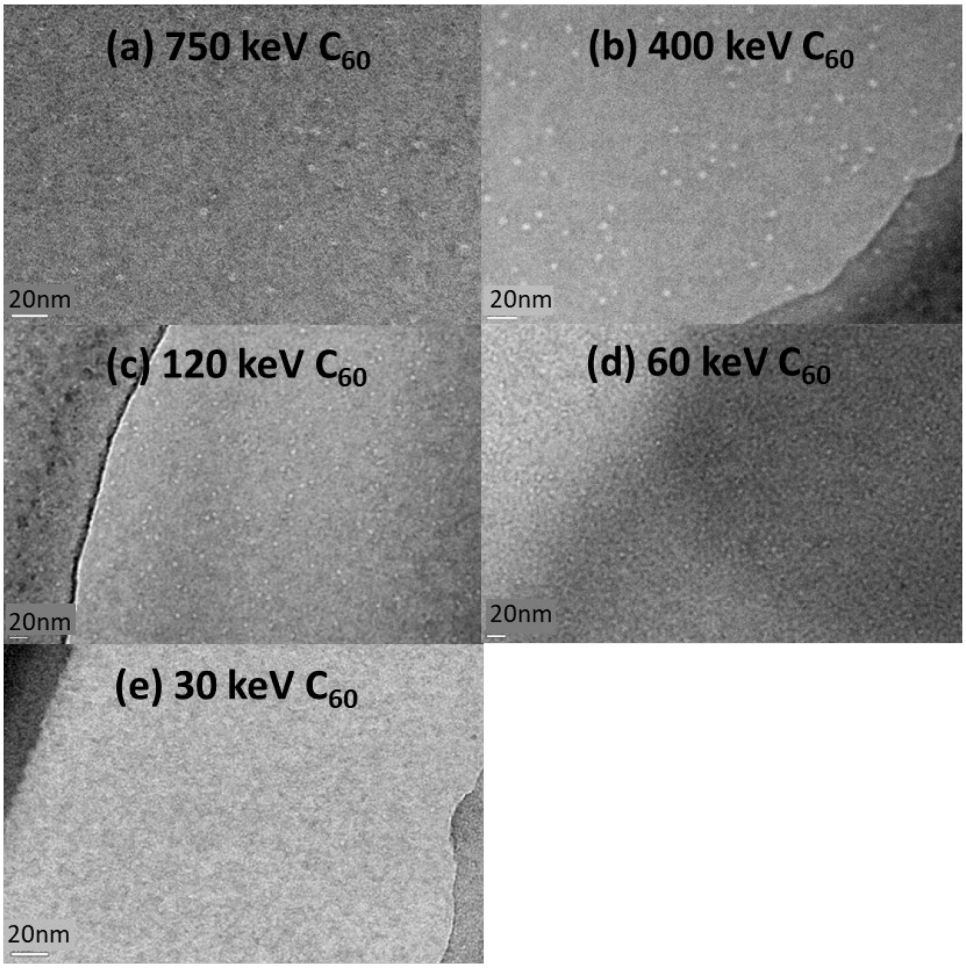

Fig. 2. Top-view BF-TEM images of ion tracks in Si, which were formed with C_{60} ion irradiation of energies of 750–30 keV. The samples were irradiated to a fluence of 1×10^{11} C_{60}/cm^2 except to 5×10^{10} C_{60}/cm^2 at 750 keV. The ion tracks are indicated as white dots. Tracks were not detected at 30 keV.

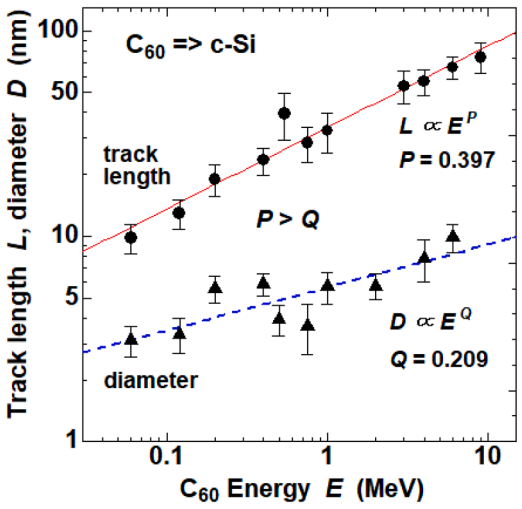

Fig. 3. Ion energy (E) dependence of the mean track length (L, circles) and mean diameter (D, triangles) in Si irradiated with C_{60} ions, determined from the side- and top-view TEM images, respectively. The circles (triangles) and bars show the mean values ± standard deviations, respectively. The solid and broken lines indicate the least squares fitting of the power laws of $L \propto E^{0.397}$ and $D \propto E^{0.209}$, respectively.

The exponent of the track length L ($P = 0.397$), exceeded that of diameter D ($Q = 0.209$). Thus, L increased more steeply than D. Considering that the AR is defined as L/D,

$$AR = L/D \sim E^{P-Q} \sim E^{0.188}. \quad (8)$$

The AR increased with an increase in E, as confirmed in Fig. 1. The tracks formed at higher (lower) energies exhibited shapes with a higher (lower) AR.

In our previous publication [11], high resolution TEM (HR-TEM) observation was applied to a Si sample irradiated with 6 MeV C_{60} ions. A damaged crystalline track, but not amorphous, was observed. However, it needs caution to perform this kind of observation, because the film thickness should thinner than the track length [26], hopefully less than (the mean track length) − 2 × (SD). Otherwise, an amorphous track shows lattice fringes from deeper crystalline layer than the track length [26]. Therefore, this kind of observation is not easily applicable to samples irradiated with lower energy C_{60} ions than 6 MeV. To confirm the damage crystalline nature of the ion tracks formed by 6 MeV C_{60} ions, Rutherford backscattering spectrometry/Channeling (RBS/C) measurements were conducted and have supported the HR-TEM result [11].

4. Discussion

4.1. Nonelectronic contribution to track formation

Fig. 4 shows the S_e dependence of the squared mean track radii, i.e., R^2. We previously reported [9,11] that the R^2 between 1 and 9 MeV was well fitted with an empirical law [31]:

$$R^2 = C(S_e - S_{e,th}) \quad (9)$$

where C and $S_{e,th}$ indicate a proportional coefficient and S_e threshold of 4.2 keV/nm, respectively. This empirical law is indicated by a broken line in Fig. 4. The solid curve represents the S_e dependence of the R^2 calculated from the inelastic thermal spike (i-TS) model while assuming the melting criterion [6]. The i-TS curve slightly overestimated the track radii, possibly because the partial recrystallization of the tracks in Si [8] was not presumed in the i-TS model. However, the extrapolated threshold from the i-TS curve was comparable with that from the

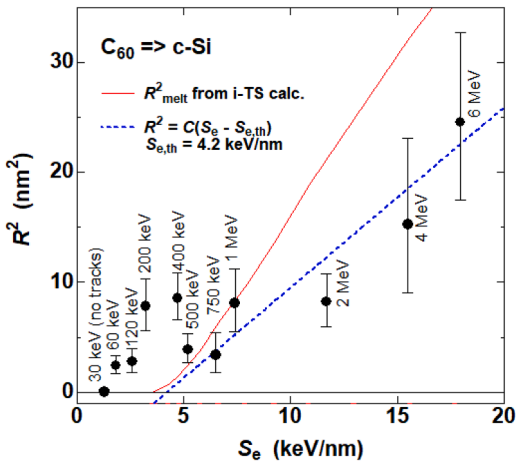

Fig. 4. Squared mean track radii (R^2) versus electronic energy deposition (S_e) of C_{60} ions in Si. The circles and bars show the mean values ± standard deviations, respectively. The broken line indicates the empirical rule of $R^2 = C(S_e - S_{e,th})$, which was optimized with data between 1 and 9 MeV [11]. The solid curve indicates the S_e dependence of R^2 calculated from the inelastic thermal spike (i-TS) model [6].

empirical law (Eq. (9)). Both curves vanished around ~4 keV/nm. Hereinafter, the extrapolated threshold is described as ~4 keV/nm. C_{60} ions of 60, 120, and 200 keV afforded S_e values of 1.8, 2.6, and 3.2 keV/nm, respectively, i.e., all of them were below the threshold of ~4 keV/nm. Even if they were below the S_e threshold, the tracks were experimentally confirmed under 60-, 120-, and 200-keV irradiation.

Fig. 5 shows the ion energy dependence of the track diameter and energy losses. The dependence of the diameter between 750 keV and 9 MeV was consistent with that of the S_e (solid curve). However, the decrease in the diameter slowed at 500 keV, whereas the S_e decreased more steeply. Around 300 keV, the S_e decreased to the threshold value of ~4 keV/nm, which was determined from an extrapolation in Fig. 4. As previously described, the track formation below 300 keV could not be attributed to the S_e only. To compensate for the decrease in the S_e with a decrease in energy, the nuclear energy loss (S_n) increased and became more dominant than the S_e at ~700 keV and below. Larger diameters were observed at 200 and 400 keV than those at 500 keV. The compensating S_n or the synergy effect between the S_e and S_n was

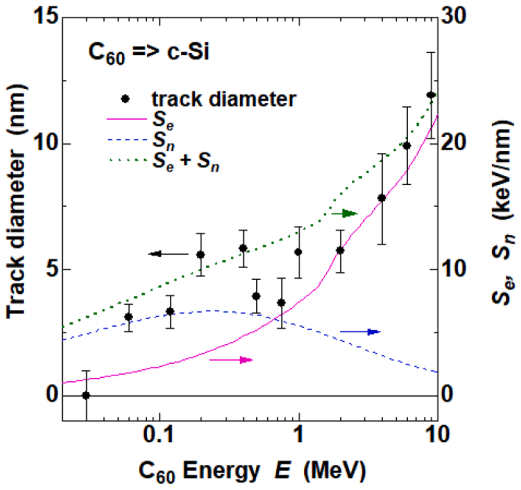

Fig. 5. The ion energy dependence of the mean track diameter in Si irradiated with C_{60} ions is shown by circles and bars, indicating the mean values ± standard deviation, respectively. The energy dependences of S_e, S_n, and (S_e + S_n), calculated from Eq. (1), are indicated by solid, broken, and dotted curves, respectively.

probably the driving force of the track formation below the S_e threshold of ~4 keV/nm. However, a preliminary unified thermal spike (u-TS) calculation predicted that the track radii should increase with decreasing the C_{60} energy from 6 MeV to 1 MeV, which was completely inconsistent with our experiments.

Some discontinuities are observed in the energy dependence of the track diameter as shown in Fig. 5, between 120 keV and 200 keV, 400 keV and 500 keV, 750 keV and 1 MeV. However, they cannot be explained by the jumps of the incident charge state of C_{60} ions: As already described in the Experimental section, the energies (the incident charge states) were 1 MeV (+1), 750 keV (+3), 500 keV (+2), 400 keV (+2), 200 keV (+1), and 120 keV (+1). While there is a jump on the track diameter from 1 MeV to 750 keV (+1 to +3), but no jump from 750 keV to 500 keV (+3 to +2). Furthermore, a jump was observed from 500 keV to 400 keV (+2 to +2), while the charge state was maintained. Moreover, a jump was not observed from 400 keV to 200 keV (+2 to +1) while the charge state changed. Again, a jump was observed from 200 keV to 120 keV (+1 to +1) while the charge state did not change.

4.2. Cluster track length and monatomic ion range

The ion energy E dependence of the mean track length L in Si is again shown in Fig. 6. Although it has already been shown in Fig. 3, L was fitted by a power law of $L \propto E^{0.379}$.

As previously mentioned, we presumed the validity of Eq. (1). Thus, the energy-loss processes of each C atom constituting a C_{60} ion were assumed the same as those of a monatomic C ion, i.e., the independent energy-loss processes of each C atom irrespective of the formation of a C_{60} molecule. One of the consequences of the independent energy-loss processes for C atoms forming a C_{60} molecule is that the ion ranges of the C atoms forming the C_{60} molecule should be comparable to those of monatomic C ions separately injected into Si. The corresponding ion range (R_p) of monatomic C ions with the same velocity as the C_{60} ions was calculated using the SRIM 2013 code [15] and shown by a broken curve in Fig. 6. The calculated R_p was considerably longer than the experimental mean track length (L) at 1 MeV or above but became shorter than L at 200 keV or below.

The R_p is the mean depth where injected ions are stopped. Contrarily, an injected ion should be so energetic within the ion track that the S_e of the ion always overcomes the track formation threshold, $S_{e,th}$. The considerably shorter track length compared with the R_p is quite common

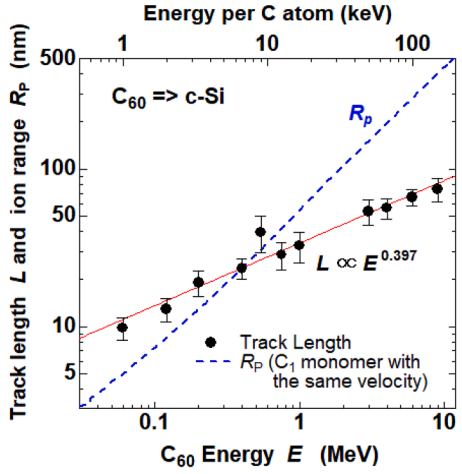

Fig. 6. The ion energy (E) dependence of the mean track length (L) in Si irradiated with C_{60} ions is shown by circles and bars, indicating the mean values ± standard deviations, respectively. The solid line indicates the least squares fitting of the power law of $L \propto E^{0.397}$. The broken curve indicates the ion range of the monatomic C ion in Si with the same velocity as the C_{60} ion, calculated using the SRIM 2013 code [15].

in different materials, such as yttrium iron garnet (YIG) [32] irradiated with MeV C_{60} ions. Dunlop et al. [32] mentioned that a difference between C_{60} ions and m-SHIs is whether the fragmentation of the ions is induced or not. If a C_{60} ion is destroyed into pieces by multiple nuclear collisions with Si atoms in the target but the distances among them are considerably shorter than the delta-electron ranges, the fragmented parts are still regarded as the same ion maintaining the track. When the distances among the fragments exceed the delta-electron ranges, the fragmented parts are no longer regarded as the same ion; thus, the track must be interrupted. The track continuity condition of the S_e threshold is applied to each fragment: i.e., the S_e of each fragment should exceed the threshold $S_{e,th}$ even after fragmentation. Thus, the track length being considerably shorter than the ion range is reasonably understood.

The R_p steeply decreased with a decrease in the ion energy (Fig. 6). The ratio of C_{60} ions that reached the R_p before being affected by the fragmentation may have increased. Thus, the track length decreased less steeply than the R_p (Fig. 6).

However, the track length being longer than the ion range observed at 200 keV or less (Fig. 6) was a bit unexpected. However, it has been observed that C atoms that form C_{60} molecular ions are implanted deeper into a solid than isolated monatomic C ions with the same velocity [25]. Morita et al. compared the ranges of the same-velocity ions of 30 keV C_{60}^+ and 0.5 keV C^+ monomer ions in Si via high-resolution Rutherford backscattering spectrometry (HR-RBS) [25]. The former and latter ranges were 6.1 and 4.0 nm, respectively. Since the experimental conditions of Morita et al. (30 keV C_{60}^+ ion irradiation to Si detected by HR-RBS) were quite similar to those of the present observations (60–200 keV C_{60}^+ ion irradiation to Si detected by TEM), the track-length enhancement observed in the present work can be ascribed to the same origin.

Morita et al. ascribed the range enhancement to "the acceleration effect" of the cluster ion irradiation [25]; i.e., the leading ions are accelerated and injected deeper by being pushed by the trailing ions [24]. Historically the range enhancement of cluster ions was discussed by Sigmund and ascribed to "the clearing-the-way (CTW) effect" [33, 34]; i.e., the leading ions clear away the target atoms for deeper injection of the trailing ions. However, the CTW effect is induced only when $M_1 > M_2$, where M_1 and M_2 denote the elemental masses of the incident and the target ions, respectively. The CTW effect is not induced when $M_1 < M_2$. Yamamura and Muramoto, however, showed that the range enhancement was induced even when $M_1 < M_2$ using Monte Carlo simulations, while the enhancement was lower compared to the case of $M_1 > M_2$ [24]. Since the CTW effect cannot explain the enhancement in the case of $M_1 < M_2$, another mechanism, i.e., the acceleration effect, was proposed [24]. Tracks longer than the ion range of isolated monatomic C ions, which were observed in the present work, were ascribed to "the acceleration effect."

4.3. Energy dependence of mean track volume

Fig. 7 shows the ion energy dependence of the mean track volume (V), which was simply determined from the mean radius (R) and L through the following relationship:

$$V = \pi R^2 L \tag{10}$$

As shown by a solid line in Fig. 7, the data points were well fitted by a power law of

$$V \propto E^{0.871}. \tag{11}$$

The exponent of 0.871 was close to unity; thus, the data points were fitted while assuming the linear law of

$$V \propto E, \tag{12}$$

as shown by a broken line in Fig. 7, which also provides excellent agreement. If the exponent can be approximated to unity, i.e., the track

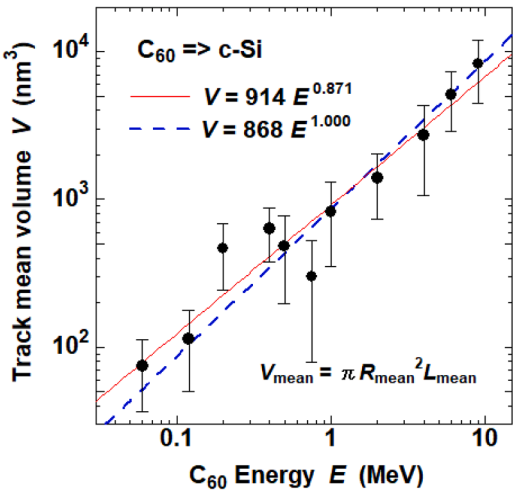

Fig. 7. Ion energy (E) dependence of the mean track volume (V) in Si irradiated with C_{60} ions. The circles and bars show the mean volumes ± standard deviations, respectively. The solid and broken lines indicate the least squares fitting of a power law of $V \propto E^{0.871}$ and linear law of $V \propto E$, respectively.

volume is assumed to be proportional to the ion energy, a significantly simpler scenario could be applied for the track formation. Aoki et al. conducted molecular dynamics (MD) simulations of the impacts of Ar cluster ions on Si surfaces, with a cluster size of 13–3000 atoms and acceleration energy of 0.5–55 keV [35]. They reported that the penetration depth of the cluster ions, which corresponds to the L in the present study, was proportional to the cubic root of the acceleration energy, i.e., $E^{1/3}$. Thus, the crater volume was linearly proportional to E.

As previously described, the track length is determined by a series of complex processes, such as the fragmentation of C_{60} molecules by multiple collisions, which increase the distance and decrease the interactions among the fragments. However, if the mean track volume, V (track length L), was assumed to be proportional to the ion energy (E) (cubic root of the energy, $E^{1/3}$), L can be easily estimated as

$$L \sim E^{1/3}. \tag{13}$$

Of course, this is not correct since the experimental results indicate that

$$L \sim E^{0.397}, \tag{14}$$

as shown in Fig. 3. However, Eq. (13) could provide a crude but useful clue to estimating L. Table 2 summarizes the power-law exponents of the track length, diameter, and volume. From the linear fitting of

$$V[nm^3] = 868E[MeV], \tag{15}$$

shown in Fig. 7, a track volume of 868 nm^3 was expected for each 1 MeV C_{60} ion, in which 8.67×10^4 bonds of Si exist. If the energy of 1 MeV was equally shared by the Si bonds in the aforementioned track volume, one bond received the energy of 11.2 eV, which was sufficient for bond rupture.

Table 2
Exponents of power-law dependences, which were assumed for the ion energy (E) dependences of the mean length (L), mean diameter (D), and mean volume (V) of the tracks.

Track length $L \propto E^P$	$P = 0.397$
Track diameter $D \propto E^Q$	$Q = 0.209$
(Aspect ratio $AR = L/D \propto E^{P\text{-}Q}$ $P > Q \rightarrow$ higher AR for higher E.)	
Track volume $V \propto E^R$	$R = 0.871$

4.4. Comparison with past studies

Shen et al. studied the damage in Si induced by 100–530 keV C_{60} ion irradiation via RBS/C measurements [36]. We evaluated track formation not only in the energy region evaluated by Shen et al. (100–530 keV) but also in a considerably wider energy region (30 keV to 9 MeV). Shen et al. irradiated to a fluence between 2×10^{11} and 5×10^{12} C_{60}/cm^2, which was slightly higher than the present study of 5×10^{10} or 1×10^{11} C_{60}/cm^2.

Fig. 5 shows the energy dependences of S_e and S_n, indicating that the S_n exceeded the S_e below 700 keV. In the region studied by Shen et al. (100–530 keV), the S_n was always higher than the S_e. However, the S_e was not negligible compared with the S_n. While Shen et al. interpreted their experimental results as efficient damage production via collision cascades and spike formation [36], the results of Shen et al. should be regarded as not a purely S_n-dominant region but S_n-dominant with a non-negligible S_e region. In fact, the present study always observed cylindrical damage regions, which can be called ion tracks at high-energy while changing the ion energy from 9 MeV (S_e-dominant region) to 60 keV (S_n-dominant). No clear transition from electronic ion tracks (cylindrical) to nuclear collision cascades (spherical) was detected.

In the previous paper [9], we discussed that tracks are formed under C_{60} irradiation, but not under m-SHIs even at the same S_e range. The i-TS model of the melting criterion including the velocity effect cannot explain the experimental results of m-SHIs [6]. Furthermore, the i-TS calculations well reproduced the S_e dependence of track diameter under MeV C_{60} ion irradiation [9], while experiments showed that tracks were not formed at the same S_e values under m-SHI irradiation.

To explain these behaviors, we extended the track recrystallization model proposed by Chadderton [8]. After m-SHI irradiation, tracks were not observed because the recrystallization of tracks had been promptly induced as proposed by Chadderton. Similar disappearance of the tracks by the recrystallization was proposed in MgO from the MD simulations [37]. We additionally assumed the track recrystallization was inhibited by defects introduced by S_n-related processes. It should be noted again that S_n delivered by C_{60} ions is much higher than that of m-SHIs. The tracks in Si are formed and stabilized by the synergy effect of S_e and S_n under C_{60} irradiation, but not by the u-TS effect.

Two other synergy effects are known [9], i.e., the pre-damage effect [31] and the u-TS model [38]. Since the tracks are formed in virgin Si samples, the pre-damage effect does not play a role in the present case. The u-TS model was applied to Si irradiated with C_{60} ions. A preliminary result showed the track diameter increased with decreasing the ion energy from 6 MeV to 1 MeV, which was completely different from our experimental observation. The u-TS model is also excluded. (The recrystallization model is not consistent with the observation of hydrogen loss from the hydrogen-terminated Si irradiated with m-SHIs [10]. We need to look for a more suitable model.)

Even taking into account the low energy behaviors in the present work, the role of S_n does not mostly change but a minor addition: As shown in Fig. 4, the squared track radii R^2 follow the relation $R^2 = C(S_e - S_{e,th})$ at 500 keV and higher, where C and $S_{e,th}$ denote the proportional constant and the S_e threshold, respectively. Since the threshold $S_{e,th}$ was ~4 keV/nm, the tracks should not be formed below this threshold. However, the tracks are formed even at 200 keV or less, which are not due to the pure-S_e origin but probably assisted by S_n.

Even at the low energies, the main role of S_n is the same as the high energies, i.e., the introduction of defects to prevent the track recrystallization. However, a minor portion of energy delivered by the S_n-related processes additively contribute to decrease the track formation threshold $S_{e,th}$.

5. Conclusions

Ion track formation in crystalline Si induced by C_{60} ion irradiation was investigated within 30–750 keV using a 400-kV single-ended ion

implanter, in addition to our previous study between 1 and 9 MeV using a 3-MV tandem accelerator [9,11]. With a decrease in the ion energy from 9 MeV, the track length and diameter decreased, although the length decreased more steeply than the diameter. Although the tracks, i.e., *localized* damaged regions, were perceived down to 60-keV irradiation, they were not observed; however, a weak *continuous* damaged region was observed under 30-keV irradiation.

The S_e threshold of the track formation was estimated using two methods: the i-TS theory and the empirical squared radius law. Although both of them suggested a S_e threshold of ~4 keV/nm, tracks were formed even at 1.8 keV/nm, i.e., below the threshold, indicating a contribution from the nuclear collisional processes.

The ion track length (L) of C_{60} ions was compared with the ion range (R_p) of monatomic C ions with the same velocity. Although the latter was longer than the former above 400 keV, the former became longer than the latter below 400 keV. The enhancement of L in the low-energy region can be attributed to "the acceleration effect" of the cluster-ion irradiation, whereas the reduction in L in the high-energy region was attributed to the fragmentation of C_{60} ions through multiple collisions with the Si matrix. The experimental results indicated that the track volume was roughly proportional to the incident C_{60} energy but not exactly. This approximated linearity could provide a crude but useful clue to estimating the track length.

Declaration of generative ai in scientific writing

No generative AI has been used in the preparation of this paper.

Preprints

An earlier version is available at SSRN: https://ssrn.com/abstract=4944996.

Funding

This work was supported by JSPS-KAKENHI Grant number 22K04990.

CRediT authorship contribution statement

H. Amekura: Conceptualization, Investigation, Writing – original draft, Writing – review & editing. **K. Narumi:** Conceptualization, Investigation, Methodology, Writing – review & editing. **A. Chiba:** Methodology, Validation. **Y. Hirano:** Methodology, Validation. **K. Yamada:** Methodology, Validation. **S. Yamamoto:** Methodology, Formal analysis. **Y. Saitoh:** Methodology, Validation.

Declaration of competing interest

The authors declare that they have no known competing financial interests or personal relationships that could have appeared to influence the work reported in this paper.

Acknowledgments

A part of the study was supported by the Inter-organizational Atomic Energy Research Program through an academic collaborative agreement among JAEA, QST, and the Univ. of Tokyo. The authors are grateful to the crew of the accelerator facilities at QST-Takasaki for their help. HA was supported by JSPS-KAKENHI Grant number 22K04990. This work was supported by "Advanced Research Infrastructure for Materials and Nanotechnology in Japan (ARIM)" of the Ministry of Education, Culture, Sports, Science and Technology (MEXT). Proposal Numbers JPMXP1223NM5040 and JPMXP1224NM5073.

References

[1] K. Suzuki, Ion Implantation and Activation, 1, Bentham Science Publishers, 2013, https://doi.org/10.2174/9781608057818113010l.
[2] M. Toulemonde, J. Dural, G. Nouet, P. Mary, J.F. Hamet, M.F. Beaufort, J. C. Desoyer, C. Blanchard, J. Auleytner, High energy heavy ion irradiation of silicon, Phys. Status Solidi (a) 114 (1989) 467–473, https://doi.org/10.1002/pssa.2211140205.
[3] P. Mary, P. Bogdanski, M. Toulemonde, R. Spohr, J. Vetter, Deep-level transient spectroscopy studies of U-irradiated silicon, Nucl. Instrum. Methods Phys. Res. Sect. B 62 (1992) 391–393, https://doi.org/10.1016/0168-583X(92)95263-Q.
[4] B. Canut, N. Bonardi, S.M.M. Ramos, S. Della-Negra, Latent tracks formation in silicon single crystals irradiated with fullerenes in the electronic regime, Nucl. Instrum. Methods Phys. Res. Sect. B 146 (1998) 296–301, https://doi.org/10.1016/S0168-583X(98)00512-6.
[5] A. Dunlop, G. Jaskierowicz, S. Della-Negra, Latent track formation in silicon irradiated by 30 MeV fullerenes, Nucl. Instrum. Methods Phys. Res. Sect. B 146 (1998) 302–308, https://doi.org/10.1016/S0168-583X(98)00509-6.
[6] A. Chettah, H. Kucal, Z.G. Wang, M. Kac, A. Meftah, M. Toulemonde, Behavior of crystalline silicon under huge electronic excitations: a transient thermal spike description, Nucl. Instrum. Methods Phys. Res. Sect. B 267 (2009) 2719–2724, https://doi.org/10.1016/j.nimb.2009.05.063.
[7] O. Osmani, I. Alzaher, T. Peters, B. Ban d'Etat, A. Cassimi, H. Lebius, I. Monnet, N. Medvedev, B. Rethfeld, M. Schleberger, Damage in crystalline silicon by swift heavy ion irradiation, Nucl. Instrum. Methods Phys. Res. Sect. B 282 (2012) 43–47, https://doi.org/10.1016/j.nimb.2011.08.036.
[8] L.T. Chadderton, Nuclear tracks in solids: registration physics and the compound spike, Radiat. Meas. 36 (2003) 13–34, https://doi.org/10.1016/S1350-4487(03)00094-5.
[9] H. Amekura, K. Narumi, A. Chiba, Y. Hirano, K. Yamada, S. Yamamoto, N. Ishikawa, N. Okubo, M. Toulemonde, Y. Saitoh, Mechanism of ion track formation in silicon by much lower energy deposition than the formation threshold, Phys. Scr. 98 (2023) 045701, https://doi.org/10.1088/1402-4896/acbbf5.
[10] C. Länger, P. Ernst, M. Bender, D. Severin, C. Trautmann, M. Schleberger, M. Dürr, Single-ion induced surface modifications on hydrogen-covered Si(001) surfaces—Significant difference between slow highly charged and swift heavy ions, New J. Phys. 23 (2021) 093037, https://doi.org/10.1088/1367-2630/ac254d.
[11] H. Amekura, M. Toulemonde, K. Narumi, R. Li, A. Chiba, Y. Hirano, K. Yamada, S. Yamamoto, N. Ishikawa, N. Okubo, Y. Saitoh, Ion tracks in silicon formed by much lower energy deposition than the track formation threshold, Sci. Rep. 11 (2021) 185, https://doi.org/10.1038/s41598-020-80360-8.
[12] L. Pelaz, L.A. Marqués, J. Barbolla, Ion-beam-induced amorphization and recrystallization in silicon, J. Appl. Phys. 96 (2004) 5947–5976, https://doi.org/10.1063/1.1808484.
[13] M.D. Mihai, D. Iancu, E. Zarkadoula, R.A. Florin, Y. Tong, Y. Zhang, W.J. Weber, G. Velişa, Athermal annealing of pre-existing defects in crystalline silicon, Acta Mater. 261 (2023) 119379, https://doi.org/10.1016/j.actamat.2023.119379.
[14] K. Tomić Luketić, M. Karlušić, A. Gajović, S. Fazinić, J.H. O'Connell, B. Pielić, B. Radatović, M. Kralj, Investigation of ion irradiation effects in silicon and graphite produced by 23 MeV I beam, Materials (Basel) 14 (2021) 1904, https://doi.org/10.3390/ma14081904.
[15] J.F. Ziegler, J.P. Biersack, M.D. Ziegler, SRIM - The Stopping and Range of Ions in Matter, SRIM Co., Chester, MD, 2008.
[16] D. Ben-Hamu, A. Baer, H. Feldman, J. Levin, O. Heber, Z. Amitay, Z. Vager, D. Zajfman, Energy loss of fast clusters through matter, Phys. Rev. A 56 (1997) 4786–4794, https://doi.org/10.1103/PhysRevA.56.4786.
[17] T. Kaneko, MeV cluster ion beam-material interaction, Quantum Beam Sci. 6 (2022) 6, https://doi.org/10.3390/qubs6010006.
[18] H. Amekura, K. Narumi, A. Chiba, Y. Hirano, K. Yamada, D. Tsuya, S. Yamamoto, N. Okubo, N. Ishikawa, Y. Saitoh, C_{60} ions of 1 MeV are slow but elongate nanoparticles like swift heavy ions of hundreds MeV, Sci. Rep. 9 (2019) 14980, https://doi.org/10.1038/s41598-019-49645-5.
[19] C. Dufour, M. Toulemonde, Models for the description of track formation, in: W. Wesch, E. Wendler (Eds.), Ion Beam Modification of Solids, vol. 61, Springer, 2016, p. 63–104, https://doi.org/10.1007/978-3-319-33561-2_2.
[20] M.P.R. Waligórski, R.N. Hamm, R. Katz, The radial distribution of dose around the path of a heavy ion in liquid water, Nucl. Tracks Radiat. Meas. 11 (1986) 309–319, https://doi.org/10.1016/1359-0189(86)90057-9.
[21] S.L. Daraszewicz, D.M. Duffy, Extending the inelastic thermal spike model for semiconductors and insulators, Nucl. Instrum. Methods Phys. Res. Sect. B 269 (2011) 1646–1649, https://doi.org/10.1016/j.nimb.2010.11.031.
[22] A. Akkerman, M. Murat, J. Barak, Ion track structure calculations in silicon – Spatial and temporal aspects, Nucl. Instrum. Methods Phys. Res. Sect. B 269 (2011) 1630–1633, https://doi.org/10.1016/j.nimb.2010.11.033.
[23] M. Murat, A. Akkerman, J. Barak, Can swift heavy ions create latent tracks in silicon? Nucl. Instrum. Methods Phys. Res. Sect. B 269 (2011) 2649–2656, https://doi.org/10.1016/j.nimb.2011.07.097.
[24] Y. Yamamura, T. Muramoto, Depth profiles due to big cluster impacts, Phys. Rev. Lett. 69 (1992) 1463–1466, https://doi.org/10.1103/PhysRevLett.69.1463.
[25] Y. Morita, K. Nakajima, M. Suzuki, K. Narumi, Y. Saitoh, W. Vandervorst, K. Kimura, Cluster effect on projected range of 30 keV in silicon, Nucl. Instrum. Methods Phys. Res. Sect. B 269 (2011) 2080–2083, https://doi.org/10.1016/j.nimb.2011.06.015.
[26] H. Amekura, A. Chettah, K. Narumi, A. Chiba, Y. Hirano, K. Yamada, S. Yamamoto, A.A. Leino, F. Djurabekova, K. Nordlund, N. Ishikawa, N. Okubo, Y. Saitoh, Latent

ion tracks were finally observed in diamond, Nat. Comm. 15 (2024) 1786, https://doi.org/10.1038/s41467-024-45934-4.
[27] S. Bouneau, A. Brunelle, S. Della-Negra, J. Depauw, D. Jacquet, Y.Le Beyec, M. Pautrat, M. Fallavier, J.C. Poizat, H.H. Andersen, Very large gold and silver sputtering yields induced by keV to MeV energy Au_n clusters ($n = 1$–13), Phys. Rev. B 65 (2002) 144106, https://doi.org/10.1103/PhysRevB.65.144106.
[28] N. Medvedev, A.E. Volkov, R. Rymzhanov, F. Akhmetov, S. Gorbunov, R. Voronkov, P. Babaev, Frontiers, challenges, and solutions in modeling of swift heavy ion effects in materials, J. Appl. Phys. 133 (2023) 100701, https://doi.org/10.1063/5.0128774. Sec. IIa.
[29] M. Toulemonde, Irradiation by swift heavy ions: influence of the non-equilibrium projectile charge state for near surface experiments, Nucl. Instrum. Methods Phys. Res. Sect. B 250 (2006) 263–268, https://doi.org/10.1016/j.nimb.2006.04.163.
[30] K. Shima, T. Ishihara, T. Mikumo, Empirical formula for the average equilibrium charge-state of heavy ions behind various foils, Nucl. Instrum. Methods Phys. Res. 200 (1982) 605–608, https://doi.org/10.1016/0167-5087(82)90493-8.
[31] A. Kamarou, W. Wesch, E. Wendler, A. Undisz, M. Rettenmayr, Radiation damage formation in InP, InSb, GaAs, GaP, Ge, and Si due to fast ions, Phys. Rev. B 78 (2008) 054111, https://doi.org/10.1103/PhysRevB.78.054111.
[32] A. Dunlop, G. Jaskierowicz, J. Jensen, S. Della-Negra, Track separation due to dissociation of MeV C_{60} inside a solid, Nucl. Instrum. Methods Phys. Res. Sect. B 132 (1997) 93–108, https://doi.org/10.1016/S0168-583X(97)00390-X.
[33] P. Sigmund, Interplay between computer simulation and transport theory in the analysis of ion-beam-induced collision processes in solids, J. Vac. Sci. Technol. A 7 (1989) 585–597, https://doi.org/10.1116/1.575894.
[34] P. Sigmund, Collision cascades and sputtering induced by Larger cluster ions, J. Phys. Colloques 50 (1989) C2.175–C172.182, https://doi.org/10.1051/jphyscol:1989230.
[35] T. Aoki, J. Matsuo, Z. Insepov, I. Yamada, Molecular dynamics simulation of damage formation by cluster ion impact, Nucl. Instrum. Methods Phys. Res. Sect. B 121 (1997) 49–52, https://doi.org/10.1016/S0168-583X(96)00698-2.
[36] H. Shen, C. Brink, P. Hvelplund, S. Shiryaev, P. Shi, J.A. Davies, Fullerene ion (C_{60}^{+}) damage in Si at 25 °C, Nucl. Instrum. Methods Phys. Res. Sect. B 129 (1997) 203–206, https://doi.org/10.1016/S0168-583X(97)00286-3.
[37] R.A. Rymzhanov, N. Medvedev, J.H. O'Connell, A. Janse van Vuuren, V. A. Skuratov, A.E. Volkov, Recrystallization as the governing mechanism of ion track formation, Sci. Rep. 9 (2019) 3837, https://doi.org/10.1038/s41598-019-40239-9.
[38] M. Toulemonde, W.J. Weber, G. Li, V. Shutthanandan, P. Kluth, T. Yang, Y. Wang, Y. Zhang, Synergy of nuclear and electronic energy losses in ion-irradiation processes: the case of vitreous silicon dioxide, Phys. Rev. B 83 (2011) 054106, https://doi.org/10.1103/PhysRevB.83.054106.